Anja Böhm,[1,2,3] Christoph Hoffmann,[1] Martin Irmler,[4] Patrick Schneeweiss,[5] Günter Schnauder,[1] Corinna Sailer,[1,2,3] Vera Schmid,[1] Jens Hudemann,[5] Jürgen Machann,[3,6] Fritz Schick,[3,6] Johannes Beckers,[3,4,7] Martin Hrabě de Angelis,[3,4,7] Harald Staiger,[1,2,3] Andreas Fritsche,[1,2,3] Norbert Stefan,[1,2,3] Andreas M. Nieß,[5] Hans-Ulrich Häring,[1,2,3] and Cora Weigert[1,2,3]

TGF-β Contributes to Impaired Exercise Response by Suppression of Mitochondrial Key Regulators in Skeletal Muscle

Diabetes 2016;65:2849–2861 | DOI: 10.2337/db15-1723

A substantial number of people at risk of developing type 2 diabetes could not improve insulin sensitivity by physical training intervention. We studied the mechanisms of this impaired exercise response in 20 middle-aged individuals at high risk of developing type 2 diabetes who performed 8 weeks of controlled cycling and walking training at 80% individual Vo_2 peak. Participants identified as nonresponders in insulin sensitivity (based on the Matsuda index) did not differ in preintervention parameters compared with high responders. The failure to increase insulin sensitivity after training correlates with impaired upregulation of mitochondrial fuel oxidation genes in skeletal muscle, and with the suppression of the upstream regulators PGC1α and AMPKα2. The muscle transcriptomes of the nonresponders are further characterized by the activation of transforming growth factor (TGF)-β and TGF-β target genes, which is associated with increases in inflammatory and macrophage markers. TGF-β1 as inhibitor of mitochondrial regulators and insulin signaling is validated in human skeletal muscle cells. Activated TGF-β1 signaling downregulates the abundance of PGC1α, AMPKα2, the mitochondrial transcription factor TFAM, and mitochondrial enzymes. Thus, the data suggest that increased TGF-β activity in skeletal muscle can attenuate the improvement of mitochondrial fuel oxidation after training and contribute to the failure to increase insulin sensitivity.

Type 2 diabetes has become an epidemic, with more than 350 million affected people worldwide. The importance of physical activity to prevent or ameliorate the diabetic metabolic state and its consequences is well accepted, and regular exercise is recommended in both the prevention and treatment of type 2 diabetes (1–3). When performed regularly, it increases whole-body fat oxidation and insulin sensitivity (4–6). However, evidence is accumulating that differences exist in the individual response to exercise training. On average, approximately 15–20% of people failed to improve their glucose tolerance and insulin sensitivity after exercise training interventions (7); this nonresponse is not restricted to a specific type of exercise (endurance or resistance training or combinations), although differences are reported (8–11).

The molecular basis for this individual response to exercise intervention is unclear. Genome-wide linkage scans performed in the HERITAGE family study underline the importance of genetic factors for the individual response of metabolic parameters to exercise (12,13). We hypothesize

[1]Division of Endocrinology, Diabetology, Angiology, Nephrology, Pathobiochemistry and Clinical Chemistry, Department of Internal Medicine IV, University Hospital Tübingen, Tübingen, Germany
[2]Institute for Diabetes Research and Metabolic Diseases of the Helmholtz Zentrum München, University of Tübingen, Tübingen, Germany
[3]German Center for Diabetes Research (DZD), Neuherberg, Germany
[4]Institute of Experimental Genetics, Helmholtz Zentrum München, German Research Center for Environmental Health (GmbH), Neuherberg, Germany
[5]Department of Sports Medicine, University Hospital Tübingen, Tübingen, Germany
[6]Section on Experimental Radiology, Department of Diagnostic and Interventional Radiology, University Hospital Tübingen, Tübingen, Germany
[7]Institute of Experimental Genetics, Center of Life and Food Sciences Weihenstephan, Technische Universität München, Freising-Weihenstephan, Germany
Corresponding author: Cora Weigert, cora.weigert@med.uni-tuebingen.de.

Received 18 December 2015 and accepted 23 June 2016.
This article contains Supplementary Data online at http://diabetes.diabetesjournals.org/lookup/suppl/doi:10.2337/db15-1723/-/DC1.

that the individual response is related to specific transcriptional signatures after training intervention that elucidate the relevant changes in muscle gene expression pattern that are linked to the improvement of insulin sensitivity. Moreover, whole-genome expression signatures can indicate the molecular mechanisms responsible for the lack of improvement in metabolic parameters after exercise training. To this end, we studied the training intervention outcome of 20 individuals at high risk for type 2 diabetes. We assessed insulin sensitivity using the surrogate Matsuda insulin sensitivity index (ISI) (14), anthropometric and clinical parameters, and physical fitness before and after 8 weeks of supervised endurance training. Insulin sensitivity high responders (HREs) and nonresponders (NREs) were determined based on the fold change in insulin sensitivity before and after the intervention. Whole-genome microarray analysis of skeletal muscle biopsies obtained before and after training was performed. These data suggested that enhanced transforming growth factor (TGF)-β1 signaling can be a negative regulator of exercise response, and this role was further investigated in primary human skeletal muscle cells.

RESEARCH DESIGN AND METHODS

Study Participants and Phenotyping

Twenty middle-aged (mean 46.4 ± 11.0 years; Supplementary Table 1) and sedentary (<2 h habitual physical activity per week; mean $V\text{O}_{2\text{peak}}$ (bike) 22.9 ± 5.1 mL/min/kg; Supplementary Table 1) individuals at high risk for type 2 diabetes were recruited. They met at least one of the following inclusion criteria: BMI >27 kg/m^2, family history (first-degree) of type 2 diabetes, or former gestational diabetes. Severe diseases were excluded using routine laboratory tests and physical examination. Insulin sensitivity (ISI) before and after the intervention was determined using a 75-g oral glucose tolerance test and calculated by the method described by Matsuda and DeFronzo (14). Routine clinical chemical parameters were measured with the ADVIA 1650 clinical chemical analyzer; insulin was analyzed with the ADVIA Centaur immunoassay system (both Siemens Healthcare Diagnostics, Fernwald, Germany). Body fat mass and distribution were determined by magnetic resonance imaging (15). Informed written consent was given by all individuals; the study protocol was approved by the ethics committee of the University of Tübingen and was in accordance with the Declaration of Helsinki.

Exercise Test and Training Intervention

Before and after the training period, all participants underwent lactate diagnostics and maximal spiroergometry, an incremental cycling test using an electromagnetically braked bicycle ergometer (Excalibur Sport; Lode BV, Groningen, the Netherlands), and an incremental walking test on a motor-driven treadmill ergometer (Saturn 2.0 and Pulsar 4.0; HP-Cosmos, Traunstein, Germany) to determine individual lactate threshold (individual anaerobic threshold [IAT]) and $V\text{O}_{2\text{peak}}$ (Table 1). The test was terminated at volitional exhaustion or muscular fatigue. IAT was defined according to Roecker et al. (16). Peak $V\text{O}_2$ was defined as the mean $V\text{O}_2$ over the last 20 s before the cessation of exercise and was assessed by metabolic gas analysis (MetaLyzer 3B and MetaMax 3B; Cortex Biophysics GmbH, Leipzig, Germany).

The training program lasted 8 weeks and consisted of three supervised exercise sessions per week. Each training session consisted of 30 min of bicycle ergometer exercise and 30 min walking on a treadmill. The training intensity was individually set at 80% of the $V\text{O}_{2\text{peak}}$ determined in the performance test before the intervention and was not changed throughout the training period. Training intensity was controlled by heart rate and estimated as energy expenditure (kilojoules per kilogram per minute) according to Péronnet and Massicotte (17).

Muscle Biopsies and Microarray Analysis

Muscle biopsies were taken from the lateral portion of the vastus lateralis of the quadriceps femoris after local anesthesia (2% Scandicaine; AstraZeneca, Wedel, Germany) before and after the training period, under sterile conditions using a fine-needle punch biopsy technique (Peter Pflugbeil GmBH, Zorneding, Germany). Snap-frozen human muscle biopsies were homogenized using a TissueLyser II (Qiagen, Hilden, Germany). Total RNA was isolated, including DNase digestion, using the miRNeasy Mini kit (Qiagen). The Agilent 2100 Bioanalyzer was used to assess RNA quality, and only high-quality RNA (RNA integrity number >7) was used for microarray analysis. Total RNA (30 ng) was amplified using the Ovation Pico WTA System V2 in combination with the Encore Biotin Module (Nugen). Amplified cDNA was hybridized on Affymetrix Human Transcriptome Array 2.0 (Affymetrix, Santa Clara, CA). Staining and scanning were done according to the Affymetrix protocol, including minor modifications as suggested in the Encore Biotin protocol. RNA was not available of one subject of the NRE group. One sample (from the HRE group) was excluded from the analysis because of low-quality data. Array data have been submitted to the Gene Expression Omnibus (GSE72462).

Materials and Reagents

Recombinant TGF-β1 protein, and TGF-β1 and platelet factor 4 (PF4) ELISAs, were from R&D Systems (Minneapolis, MN), TGF-β–inducible protein (TGFBI) ELISA was from Abcam (Cambridge, UK). Cell culture media and supplements were from Lonza (Basel, Switzerland); chicken embryo extract was from Seralab (West Sussex, UK). Antibodies against ATP5A (ab110273) and GAPDH (ab8245) were from Abcam; against AMPKα2 (07–363), from Upstate Biotechnology (Lake Placid, NY); against phospho-Ser-473 and phospho-Thr-308 of Akt (9271 and 9275) and RPS6 (2217), from Cell Signaling Technology (Frankfurt, Germany); and against Akt (610861), from BD Biosciences (Heidelberg, Germany).

Table 1—Participants' parameters before and after the intervention

	HRE (n = 8 [6f, 2m])			Intermediate group (n = 4 [2f, 2m])			NRE (n = 8 [5f, 3m])			HRE vs. NRE	
	Before	After	P*	Before	After	P*	Before	After	P*	Time × group (P1†)	Before (P2‡)
ISI OGTT ($10^{19}L^2/mol^2$)	7.1 ± 6.8	11.8 ± 11.0	0.002	7.8 ± 1.3	7.8 ± 1.0	0.8	9.8 ± 7.7	8.0 ± 5.6	0.016	<0.0001	0.4
IAT (W/kg)											
Bike	1.1 ± 0.4	1.3 ± 0.4	0.004	1.2 ± 0.3	1.4 ± 0.4	0.007	1.1 ± 0.2	1.2 ± 0.3	0.0006	0.9	1.0
Treadmill	0.9 ± 0.3	1.0 ± 0.3	0.004	1.1 ± 0.3	1.2 ± 0.3	0.07	0.9 ± 0.1	1.0 ± 0.1	0.003	0.5	0.6
V_{O_2} peak											
Bike (mL/min)	2.04 ± 0.68¶	2.25 ± 0.51	0.09	2.37 ± 0.53	2.54 ± 0.35‖	0.5	2.26 ± 0.62	2.42 ± 0.74¶	0.5	0.4	0.9
Bike (mL/min/kg)	22.3 ± 7.0¶	26.1 ± 6.8	0.09	24.4 ± 4.3	25.7 ± 2.9‖	0.5	22.7 ± 3.9	24.4 ± 5.9¶	0.5	0.4	0.7
Treadmill (mL/min)	2.2 ± 0.7	2.3 ± 0.5	0.3	3.0 ± 0.3	2.3 ± 0.2**	—	2.5 ± 0.5	2.6 ± 0.7	0.2	1.0	0.3
Treadmill (mL/min/kg)	25.2 ± 7.2	26.9 ± 6.7	0.3	30.7 ± 2.2	25.2 ± 1.0**	—	25.3 ± 3.5	27.0 ± 4.7	0.1	0.9	0.8
Age (years)	51.6 ± 10.0	51.6 ± 10.0	—	41.0 ± 10.7	41.0 ± 10.7	—	43.8 ± 11.2	43.8 ± 11.2	—	—	0.2
BMI (kg/m^2)	32.0 ± 6.0	31.6 ± 6.1	0.05	31.6 ± 1.9	31.5 ± 2.1	0.8	33.4 ± 4.6	33.1 ± 4.8	0.3	0.7	0.6
Total adipose tissue (kg)	33 ± 12	32 ± 12	0.05	35 ± 5	34 ± 5	0.4	38 ± 12¶	38 ± 12¶	0.4	0.3	0.4
Visceral adipose tissue (kg)	3.8 ± 0.7	3.6 ± 1.0	0.2	5.1 ± 2.4	5 ± 2.1	0.7	5.6 ± 4.7¶	5.4 ± 4.6¶	0.7	0.4	1.0
Lean body mass (kg)	53.7 ± 12.6¶	55.7 ± 13.3§	0.4	69.6 ± 19.5	63.6 ± 13.6‖	0.3	60.2 ± 18.8	60.7 ± 19.0	0.3	0.9	0.5
Blood pressure (mmHg)											
Systolic	130 ± 18	130 ± 8	0.9	141 ± 14	135 ± 21	0.3	139 ± 16	129 ± 1 0	0.024	0.1	0.2
Diastolic	92 ± 11	91 ± 8	0.8	92 ± 12	88 ± 12	0.4	92 ± 10	84 ± 8	0.017	0.1	1.0
Heart rate (min^{-1})	80 ± 14	70 ± 6	0.038	68 ± 11	70 ± 15	0.4	76 ± 11	71 ± 10	0.1	0.4	0.6
Glucose (mmol/L)											
At baseline	5.6 ± 0.5	5.6 ± 0.6	0.8	5.4 ± 0.3	5.5 ± 0.5	0.4	5.7 ± 0.5	5.8 ± 0.6	0.4	0.4	0.8
At 120 min	7.1 ± 1.4	6.0 ± 1.1	0.023	6.1 ± 0.6	5.6 ± 0.6	0.043	6.2 ± 0.7	7.0 ± 1.1	0.09	0.0037	0.1
Free fatty acids (μmol/L)	719 ± 200¶	532 ± 195	0.1	469 ± 171	517 ± 169	0.7	550 ± 79	590 ± 149	0.6	0.1	0.1
Triglycerides (mg/dL)	114 ± 39	81 ± 31	0.0004	135 ± 21	118 ± 53	0.5	103 ± 37	105 ± 32	0.6	0.0003	0.6
HDL cholesterol (mg/dL)	49 ± 12	49 ± 11	0.8	37 ± 8	41 ± 5	0.2	50 ± 10	48 ± 11	0.038	0.1	0.8
LDL cholesterol (mg/dL)	118 ± 22	108 ± 19	0.021	104 ± 21	103 ± 29	0.6	124 ± 35	120 ± 29	0.4	0.2	0.8
Leukocytes (1/μL)	5,944 ± 934	5,904 ± 2,076	0.6	6,190 ± 1,767	6,045 ± 1,454	0.8	6,575 ± 2,412	6,180 ± 1,528	0.6	0.9	0.7
CRP (mg/dL)	0.3 ± 0.2	0.6 ± 1.1	0.3	0.1 ± 0.1	0.1 ± 01	0.6	0.2 ± 0.3	0.4 ± 0.5	0.2	0.6	0.5

Data represent means ± SD. Before statistical analysis, data were $\log_e$-transformed to approximate normal distribution. *Paired t test. †Multivariate ANOVA, time × group. ‡Two-sided t test, before-intervention values of HRE vs. NRE. ¶From seven subjects available. §From six subjects available. ‖From three subjects available. **From two subjects available. CRP, C-reactive protein; f, female; m, male; OGTT, oral glucose tolerance test.

Human Skeletal Muscle Cell Experiments

Skeletal muscle cells were obtained from six randomly selected donors, including four participants of the current study. Cells were grown from satellite cells obtained from percutaneous needle biopsies performed on the lateral portion of the quadriceps femoris (vastus lateralis) muscle. The donors gave informed written consent to the study. The Ethical Committee of the Tübingen University Medical Department approved the protocol. CD56-positive myoblasts were isolated using MACS microbeads (Milteny Biotech, Bergisch Gladbach, Germany) and grown on six-well plates coated with Geltrex (Life Technologies, Frankfurt, Germany) in a 1:1 mixture of α-minimum essential medium and Ham's F-12 supplemented with 20% FBS, 1% chicken extract, 100 U/mL penicillin, 100 μg/mL streptomycin, and 0.5 μg/mL amphotericin B until 70–80% confluence. TGF-β1 treatment was started at day 1 (for 7 days) or day 4 (for 3 days) of fusion; cells were fused in α-minimum essential medium containing 5.5 mmol/L glucose with 2% FBS, 2 mmol/L glutamine, 125 μmol/L palmitate, 125 μmol/L oleate, 100 μmol/L L-carnitine, 100 U/mL penicillin, 100 μg/mL streptomycin, and 0.5 μg/mL amphotericin B. RNA and proteins were isolated using the NucleoSpin miRNA Kit (Macherey Nagel, Düren, Germany).

Quantitative PCR Analysis

RNA was transcribed by RT-PCR, with random hexamer and oligo-dT primers mixed using the Transcriptor First Strand cDNA Synthesis kit (Roche, Mannheim, Germany). Quantitative real-time PCR (qPCR) was performed on a Roche Lightcycler 480 using QuantiTect Primer Assays (Qiagen, Hilden, Germany) (Table 2).

Western Blotting

Protein concentration was quantified with the protein quantification assay (Macherey Nagel, Düren, Germany). Proteins were separated by sodium dodecyl sulfate polyacrylamide (7.5–15%) gradient gel electrophoresis and were transferred onto a nitrocellulose membrane by semi-dry electroblotting. Immunodetection was performed as recently described (18).

Table 2—Primer used for qPCR

Gene symbol	Catalog number or sequence
COL1A2	forward: CTC CAA GGA CAA GAA ACA CGT C reverse: ATG TTC TGA GAG GCA TAG TTG GC
CD68	QT00037184
CPT1B	QT00057036
HADHA	QT00091721
MYH2	QT00082495
MYH7	QT00000602
PPARGC1A	QT00095578
PRKAA2	QT00042077
SLC2A4	QT00097902
TBP	QT00000721
TFAM	QT00012782
TGFBI	QT01009477

Primers for *COL1A2* were designed in house. QT, Quantitect Primer Assays (Qiagen, Hilden, Germany).

Immunostaining

Cells grown on cover slips were washed with PBS, fixed in PBS containing 4% formaldehyde (pH 7.4) for 20 min, quenched with 150 mmol/L glycine in PBS for 10 min, and treated with 0.1% Triton X-100 for 2 min. Blocking was performed in 1% normal goat serum, 0.05% Tween 20 in PBS for 30 min. Cover slips were incubated with antibodies recognizing CD56 (5.1H11; Developmental Studies Hybridoma Bank, Iowa City, IA), major histocompatibility complex–fast (M4276), or major histocompatibility complex–slow (M8421; Sigma-Aldrich, Deisenhofen, Germany) diluted 1:100 in blocking solution for 1 h at room temperature, washed three times in PBS, and incubated with the Alexa 488–labeled secondary antibody (Invitrogen, Karlsruhe, Germany) diluted 1:250 in blocking solution for another 2 h and washed again. Nuclei were stained using TO-PRO3 (Invitrogen) before mounting in PermaFluor (Beckman Coulter, Krefeld, Germany).

ELISA

TGF-β1 and TGFBI were determined in plasma samples obtained by ELISA after an overnight fast. To correct for acute platelet activation during sample preparation, platelet factor 4 (PF4/CXCL4) was measured in parallel (19).

Statistical Analysis

For clinical data, statistical analysis was done using JMP11 (SAS Institute, Inc., Cary, NC). If not stated otherwise, a two-sided homoscedastic *t* test was performed. For time × group interaction, multivariate ANOVA was performed. A P value <0.05 was considered statistically significant. For some variables, participants had to be excluded because of incomplete data sets (before/after the intervention); if so, the number of analyzed participants was stated. If outliers were detected (using Grubbs' test [maximum normed residual test]; available from http://graphpad.com/quickcalcs/grubbs1/), the number of individuals included was stated. Differential gene regulation between HRE and NRE samples was done by applying the limma *t* test on log2 ratios (after intervention vs. before intervention; $P < 0.05$). To reduce background signals, data were filtered for linear arbitrary expression >8 in at least half of the samples. The microarray data set was analyzed by the statistical programming environment R implemented in CARMAweb (20) developed for microarray data analysis. Gene-wise testing for differential abundance at baseline or after the intervention between ISI HREs and NREs was done by the paired limma *t* test and Benjamini-Hochberg multiple testing correction (false discovery rate <10%; average abundance >8 in at least one group). Enriched KEGG pathways and gene ontology (GO) terms were identified using InCroMAP (21). Upstream

regulator analysis was generated through the use of Ingenuity Pathway Analysis (QIAGEN Redwood City, Redwood City, CA; www.qiagen.com/ingenuity).

RESULTS

Individual Response to Exercise Training

After 8 weeks of supervised training, the entire middle-aged study group achieved an increase in the IAT and oxygen uptake ($V\text{O}_{2\text{peak}}$ [bike]), and a decrease in BMI, total adipose tissue, blood pressure, resting heart rate, plasma triglycerides, and LDL cholesterol (Supplementary Table 1). Insulin sensitivity (ISI) did not increase significantly among the entire study group (8.3 ± 6.4 vs. 9.5 ± 7.8; $P = 0.1$), with a high variability in the change of ISI, ranging from 2.7-fold to 0.6-fold after the intervention. Two groups with the largest difference in the fold change of ISI (8 HREs and 8 NREs) were each stratified by the two outermost quintiles (Table 1). In the following, the terms *high responder* and *nonresponder* are used according to the different response in ISI, although NREs showed changes in other parameters after the intervention (Table 1). The HRE group had an average 1.6-fold increase in ISI, whereas the NRE group had even a small decrease of ISI (0.9-fold) after the exercise intervention (Supplementary Fig. 1). A significant interaction of response group and intervention was found for ISI, glucose (measured at 120 min), and plasma triglycerides (Table 1, *P*1 value). IAT was increased similarly in both groups (Table 1). Preintervention parameters—for example, insulin sensitivity, fitness, and age—were not different between the groups (Table 1, *P*2 value), and both groups trained with the same intensity (HRE vs. NRE: cycling, 0.33 ± 0.11 vs. 0.31 ± 0.09 kJ/kg/min [$P = 0.8$]; treadmill, 0.39 ± 0.10 vs. 0.35 ± 0.06 kJ/kg/min [$P = 0.5$]).

Impaired Upregulation of Mitochondrial Energy Metabolism Genes in ISI NREs

Transcriptome analyses of the muscle biopsies from the HRE and NRE groups taken before and after the 8-week training intervention revealed the differential regulation of 469 genes after training ($P < 0.05$; ratio of fold changes, >1.2 times). Significantly enriched GO terms were dominated by cellular functions and components related to mitochondria and metabolic pathways located in the mitochondrial matrix, in particular fatty acid β-oxidation, tricarboxylic acid cycle, oxidative phosphorylation, and respiratory electron transport chain (Fig. 1*A*). The transcripts of these mitochondrial enzymes and carriers located in the inner mitochondrial membrane showed impaired upregulation in the NRE group compared with the HRE group, for example, the β-oxidation enzymes carnitine palmitoyltransferase (*CPT1B*) and hydroxyacyl-CoA dehydrogenases (*HADH*) and ATP synthase (*ATP5*). Similarly, GLUT4 (*SLC2A4*) and enzymes of glucose catabolism were not upregulated in the NRE group compared with the HRE group (Fig. 1*A*), suggesting not only impaired improvement of fatty acid oxidation capacity and ATP production after the intervention in NRE but also reduced upregulation of glucose uptake and oxidation. Before the intervention, the abundance of these transcripts was not different between HREs and NREs, except for *CPT1B* (0.82-fold lower in NREs; $P = 0.03$).

Ingenuity software was used to search for upstream regulators that could explain the differences in gene regulation between NREs and HREs. The data indicate impaired activation of several regulators of exercise-dependent gene expression in the skeletal muscle of NREs, namely peroxisome proliferator–activated receptor γ coactivator PGC1α (gene name *PPARGC1*), peroxisome proliferator–activated receptor transcription factors, estrogen receptors (*ESRRA*, *ESR*), and an AMPKα2 subunit (gene name *PRKAA2*) (Fig. 1*B*). *PPARGC1A* transcript abundance was slightly increased in the HRE group after training but reduced in the NRE group (Fig. 1*C*). The NRE group also showed a reduced abundance of *PRKAA2* after the intervention (Fig. 1*C*). The fold change in transcripts of *PPARGC1* and *PRKAA2* correlated with the fold change in insulin sensitivity in the entire study group (Fig. 1*D* and *E*). Abundance of transcripts was also quantified by qPCR and gave comparable results (Supplementary Tables 2 and 3). Protein abundance of AMPKα2 and of the ATP synthase subunit α (ATP5A) was significantly increased in the HRE group, whereas the increase was attenuated in the NRE group (Fig. 1*F–H*).

Increased Upregulation of Immune Response and Inflammatory Genes and TGF-β Target Genes in ISI NREs

In addition, GO terms related to immune response, inflammatory processes, and Toll-like receptor signaling were significantly enriched among differentially regulated genes in the HRE/NRE comparison. These differentially regulated transcripts were upregulated in the NRE group after the intervention and unchanged or even reduced in the HRE group (Fig. 2*A* and *B*). The transcripts are known to be highly expressed in macrophages (*CD68*, *CXCR2*, *CD14*, *TLR4*) and neutrophils (*CD97*, *CYBB*, *NCF1*), or to act as chemoattractants (*RARRES2*). The data suggest increased infiltration of macrophages and neutrophiles and enhanced inflammation in skeletal muscle of NREs after the intervention, since no difference in the abundance of transcripts was found before the intervention when comparing HREs versus NREs ($P < 0.05$; ratio, >1.2-fold).

Candidate upstream regulators specifically activated in the NRE group are mitogen-activated protein kinases, inflammatory cytokines, and TGF-β1 (gene name *TGFB1*) (Fig. 2*C*). Several TGF-β1 target genes were upregulated after the intervention and showed a negative correlation with the change in insulin sensitivity in the entire group: TGF-β-inducible protein *TGFBI*, collagens, and matrix metallopeptidases (Fig. 2*D–F* and Supplementary Fig. 2*A–C*). TGF-β1 itself was the only upstream candidate with a differential transcript abundance after the intervention; the NRE group showed slightly increased *TGFB1* abundance compared with the HRE group (1.25-fold; $P < 0.05$).

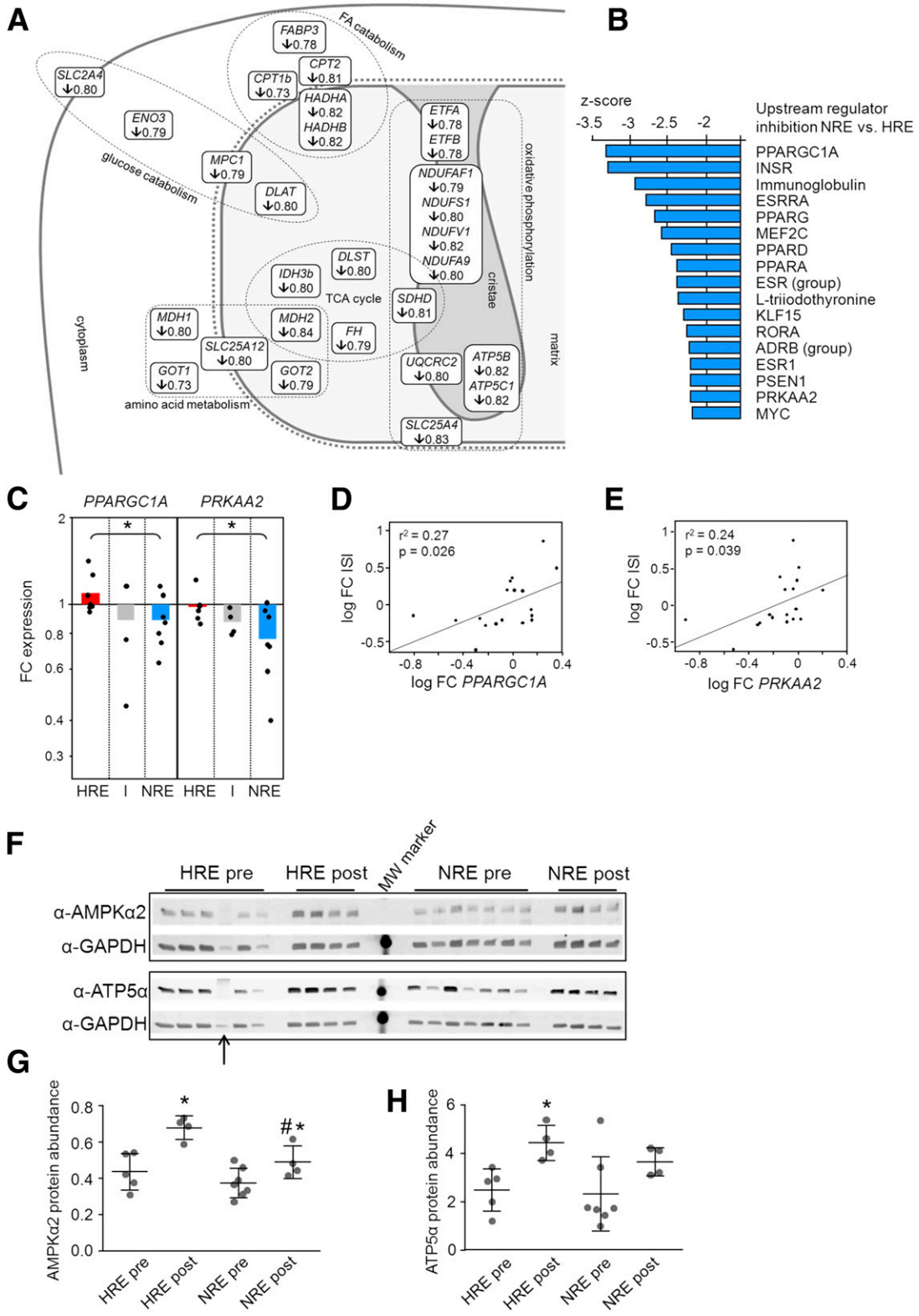

Figure 1—Impaired upregulation of mitochondrial energy metabolism genes in ISI NREs. *A*: Transcriptome analysis revealed differentially regulated genes in muscle biopsies of NREs vs. HREs after exercise related to glucose and fatty acid (FA) catabolism, amino acid metabolism, tricarboxylic acid cycle (TCA), or oxidative phosphorylation (ratio of fold changes in the comparison NRE/HRE after intervention vs. before intervention; $P < 0.05$). *B*: Upstream regulators less activated (inhibited) in NRE vs. HRE based on Ingenuity upstream regulator analysis of differentially regulated transcripts. *z*-Scores below −2 can be considered significant. *C*: Fold change (FC) after intervention vs. before intervention of *PPARGC1A* and *PRKAA2* transcripts (transcriptome data) in muscle biopsies of the participants grouped as HREs ($n = 7$), into an intermediate group (I; $n = 4$), and as NREs (NRE; $n = 7$) (Table 1). The bar graphs identify the mean of each group. *$P < 0.05$ fold change NRE vs. fold change HRE. *D* and *E*: Correlation of log-transformed fold changes in ISI and

Moreover, increased upregulation of the TGF-β receptor 2 was associated with ISI nonresponse (Fig. 2*G*). These data point to an activation of TGF-β signaling in the muscle of NREs, resulting in altered regulation of TGF-β target genes. Plasma TGF-β1, also after relation to PF4, and TGF-β-inducible protein levels were not changed after training and were not different between the HRE and NRE groups (Fig. 2*H–J*). Thus it is possible that the different activation of TGF-β signaling is restricted to the skeletal muscle of HREs and NREs.

TGF-β1 Suppresses Mitochondrial Regulators and Enzymes in Human Skeletal Muscle

TGF-β1 activity is not only dependent on its protein abundance; after secretion, the bioavailability of the active protein is regulated at multiple steps. The increase in the expression of the TGF-β1-inducible protein *TGFBI* showed a strong correlation with the upregulation of other TGF-β1 target genes in the muscle biopsies, as shown for *FN1* and *COL1A2* (Supplementary Fig. 2*D* and *E*), and thus behaves as a good readout of active TGF-β1 in skeletal muscle. Notably, the increased expression of the TGF-β1-inducible protein *TGFBI* correlated inversely with the downregulation of *PPARGC1A* and *PRKAA2* (Fig. 3*A* and *B*). Thus the muscle transcriptome data suggest a negative regulation of *PPARGC1A* and *PRKAA2* expression by TGF-β1.

We tested this hypothesis in human skeletal muscle cells. When differentiated myotubes were incubated with TGF-β1 for 24 h, we found a significant decrease in mRNA abundance in *PPARGC1A*, *PRKAA2*, the mitochondrial transcription factor *TFAM*, and key regulators of β-oxidation, *HADHA* and *CPT1B* (Fig. 3*C–G*). This decrease was prevented by cotreatment with the TGF-β receptor 1 antagonist SB431542. Treatment with SB431542 alone increased the expression of *PPARGC1A* and *CPT1B*. This effect can be a result of the inhibition of autocrine TGF-β1 activity, which is also visible as reduced expression of the TGF-β1 target gene *TGFBI* in the presence of SB431542 (Fig. 3*H*). TGF-β1 treatment of myotubes had also an inhibitory effect on insulin signaling since it reduced insulin-stimulated phosphorylation of Akt/protein kinase B (Fig. 3*I–K*). When the cells were treated with TGF-β1 for 3 or 7 days, a marked downregulation of *PPARGC1A* was observed, whereas treatment with the TGF-β receptor 1 antagonist SB431542 alone increased the expression approximately fivefold (Fig. 4*A*). TGF-β1-induced inhibition was also found for *PRKAA2*, *TFAM*, *HADHA*, and *CPT1B* expression, with an opposite effect of the antagonist SB431542 (Fig. 4*B–E*). Moreover, TGF-β1 reduced the protein abundance of both AMPKα2 and ATP5A (Fig. 4*F–H*). TGF-β1 treatment also blocked the increase in mRNA abundance of *MYH2* and *MYH7* and muscle cell differentiation (Fig. 4*I–K*). Notably, cells obtained from donors identified as ISI HREs and NREs did not differ in their response to TGF-β1 (Supplementary Fig. 3). To conclude, these data indicate that TGF-β1 downregulates the abundance of mitochondrial regulators and mitochondrial enzymes in skeletal muscle cells. This inhibitory effect is found in differentiated myotubes and during cell differentiation.

DISCUSSION

In this study we provide evidence for a molecular mechanism that can contribute to the failure to improve insulin sensitivity after an exercise intervention. Given the enormous relevance of physical activity in the prevention and therapy of type 2 diabetes, and a notable number of individuals who showed no beneficial effects of training on metabolic parameters (7), it is important to understand the molecular basis of this exercise nonresponse.

All subjects in our study improved their IAT, but they showed a huge variability in their fold change in insulin sensitivity after the eight weeks of supervised endurance training. We clearly defined a group of responders that could increase their insulin sensitivity after the training intervention and a group of NREs. Using whole-genome microarray analyses of the muscle biopsies taken before and after the intervention, we gained unbiased insight into the training-induced molecular changes in muscle of the responders and NREs.

We identified specific transcriptional profiles in the muscle of the NRE group and provide evidence from cell culture studies for a role of TGF-β1 as one negative regulator of mitochondrial activators and enzymes potentially preventing a beneficial metabolic adaptation to training. The NREs showed increased expression of TGF-β1, of the receptor *TGFBR2*, and of several target genes of TGF-β. Notably, the transcripts that indicate higher TGF-β activity were not different before the intervention. Thus this different transcriptional profile is caused by a different response to training.

In addition, the failure to improve insulin sensitivity is associated with impaired upregulation of genes that are important for glucose and fatty acid oxidation and mitochondrial oxidative phosphorylation. The transcriptional coactivator PGC1α and AMPK were identified as relevant upstream regulators that are implicated in this exercise nonresponse. Importantly, the mRNA abundance of genes encoding for PGC1α and AMPKα2 was downregulated in

fold changes in transcripts (n = 18). *F–H*: Immunoblots of protein lysates of muscle biopsies using indicated antibodies. Detection of GAPDH serves as the loading control for separate blots. Relative band intensity values normalized to GAPDH are shown (n = 4–7, mean ± SD). *P < 0.05 vs. before the intervention [pre]; #P < 0.05 HRE vs. NRE after the intervention [post]). Lanes between the before and after samples and between the samples and the molecular weight (MW) marker were empty. The lane marked with the arrow does not show any detectable ATP5α or AMPKα2 signal; hence it was excluded from quantification.

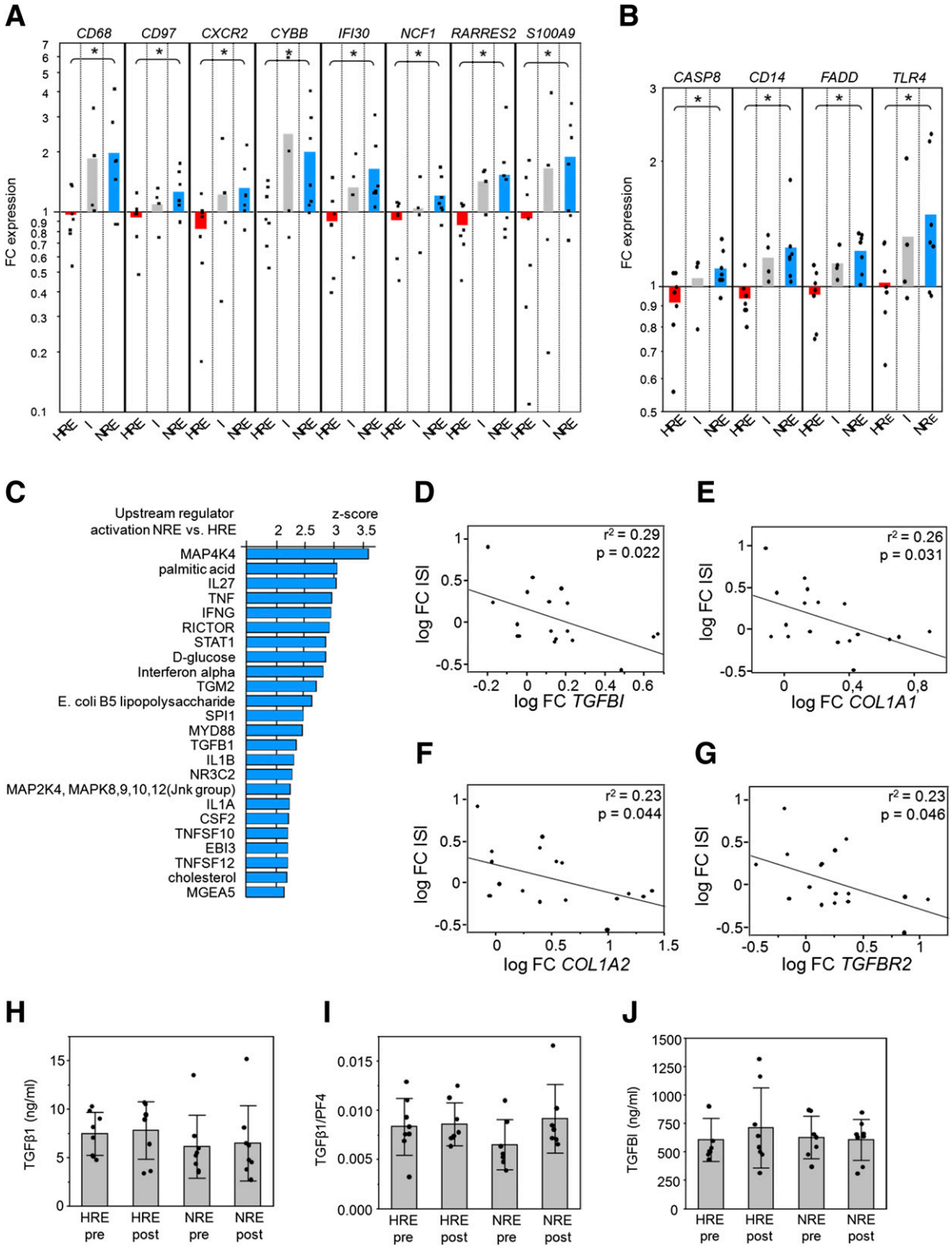

Figure 2—Increased upregulation of immune and inflammatory genes and TGF-β target genes in ISI NREs. Transcriptome analysis revealed differentially regulated genes in HREs vs. NREs after exercise, related to immune response and inflammatory processes (*A*) and Toll-like receptor signaling (*B*). Shown is the fold change (FC) after the intervention vs. before the intervention of transcripts in muscle biopsies of the participants grouped as HREs (n = 7), into an intermediate group (I; n = 4), and as NREs (NRE; n = 7) (Table 1). Bar graphs identify the mean of each group. *P < 0.05 fold change NRE vs. fold change HRE. *C*: Upstream regulators activated in NRE vs. HRE based on Ingenuity upstream regulator analysis of differentially regulated transcripts. z-Scores >2 can be considered significant. *D–G*: Correlation of log-transformed fold changes in ISI and fold changes (after intervention vs. before intervention) in TGF-β target gene and *TGFBR2* transcripts in muscle biopsies assessed by transcriptome analyses (n = 18). *H–J*: Plasma concentration of TGF-β1 (*H*), TGF-β1 related to

the muscle of NREs after the intervention. We proved a causal relationship of the increased TGF-β1 activity and the suppression of PGC1α and AMPKα2 in human skeletal muscle cells. TGF-β1 downregulated and blockade of TGF-β signaling upregulated the expression of PGC1α and AMPKα2, and consequently of the mitochondrial transcription factor *TFAM*, which is regulated by PGC1α (22). Moreover, TGF-β1 downregulated key regulators of mitochondrial fatty acid oxidation—what is likely to be a consequence of the negative effect on PGC1α and AMPK. Both proteins are key players in the exercise-dependent regulation of enzymes involved in fuel oxidation (23). Thus the cell culture data provide clear evidence for the molecular mechanism suggested by the transcriptome analyses of the muscles of responders and NREs.

On a molecular level, activation of TGF-β1 signaling leads to phosphorylation of SMAD3, which can act as a transcriptional repressor at the PGC1α promoter (24). The importance of the TGF-β/SMAD3 pathway for metabolic control in humans is suggested by a close association of BMI and circulating TGF-β1 levels (25), and the association of elevated plasma TGF-β1 and higher risk for type 2 diabetes (26). A rat model with insulin resistance and a low aerobic response to exercise shows increased activation of SMAD3-dependent gene expression after an acute exercise bout when compared with rats with a high aerobic response (27). Although the causal relationship needs to be proven in vivo, these data point to chronically elevated TGF-β1 activity as a negative regulator in the adaptation of fuel oxidation in response to training, demonstrated for the first time in a human exercise intervention study. The TGF-β-mediated inhibition of skeletal muscle differentiation, as shown in the human muscle cells in our study and described earlier (28), can play an additional role here.

While all participants in our study were untrained and overweight, only some of them showed an adverse response to the training intervention. The increased expression of markers of macrophages, neutrophils, and inflammation suggests local inflammatory processes in the muscle of these NREs, even though increased recruitment of immune cells was not investigated by immunohistochemistry in our study. Activated resident macrophages and infiltrated immune cells release TGF-β, which is a physiological response of the skeletal muscle to mechanical loading and is involved in the synthesis and reorganization of extracellular matrix components (29). The recruitment of macrophages and neutrophils is often associated with acute eccentric or resistance exercise (30), but it can also occur after endurance exercise (31). TGF-β then activates fibroblasts in the muscle to produce extracellular matrix proteins and TGF-β itself (32), while muscle satellite cells and myofibers may contribute to the enhanced production of TGF-β and extracellular matrix proteins (33,34). This process possibly took place in all participants of our study after the first training sessions, as part of the normal regeneration program of an untrained muscle (32,35). Since the training intensity was comparable between the HRE and NRE groups, higher intensity cannot explain the increased expression of inflammatory markers and TGF-β target genes in the muscle of NREs. It is more likely that the adaptation process after the unaccustomed physical activity is different. This indicates the importance of carefully designed, individualized training protocols for physically inactive subjects to avoid the possible consequences of unaccustomed skeletal muscle activity. On the other hand, we cannot rule out the possibility that the duration or intensity of our training protocol was not conducive for the metabolic improvement of some of our study participants. Extension of the training period with reduced exercise intensity or a combination of high-intensity training and resistance training might be a way to overcome the lack of metabolic improvement. A limitation of our study is the self-determined order of the exercise type (walking/cycling) in each training session. The order was not recorded and might have influenced the training outcome. Moreover, we do not know whether the muscle used for the biopsies was similarly recruited during walking and cycling in all subjects.

Clearly, increased TGF-β activity is only one potential contributor to the individual exercise response. An interesting upstream regulator candidate with a high activation score in the NRE group compared with HRE group, which we did not further investigate in this study, is the mitogen-activated protein kinase kinase kinase kinase 4 (MAP4K4). MAP4K4 deficiency in skeletal muscle of mice improves insulin sensitivity and protects from obesity-induced insulin resistance (36), and genetic polymorphisms in the *MAP4K4* locus have been associated with insulin resistance (37). Thus activation of this kinase in skeletal muscle may be another regulator of the individual differences in the metabolic response to training interventions.

Our data underline the importance of PGC1α for the beneficial effects of exercise on metabolic control. PGC1α is considered as an important upstream regulator of training-induced metabolic adaptations because of its potency to activate mitochondrial biogenesis and the formation of oxidative muscle fibers (22,38,39). In addition, genetic variations in the *PPARGC1A* gene were associated with the change in insulin sensitivity and fitness after a 9-month lifestyle intervention (40). Our results are also well in accordance with a recent study that showed that only individuals who achieved normalized glucose tolerance after exercise training

the plasma concentration of PF4 (*I*), and TGFBI (*J*) in HRE samples (n = 8) and NRE samples (n = 8) before (pre) and after (post) 8 weeks of training intervention. Individual concentrations are shown as black dots. The bar graphs identify the mean ± SD of each group.

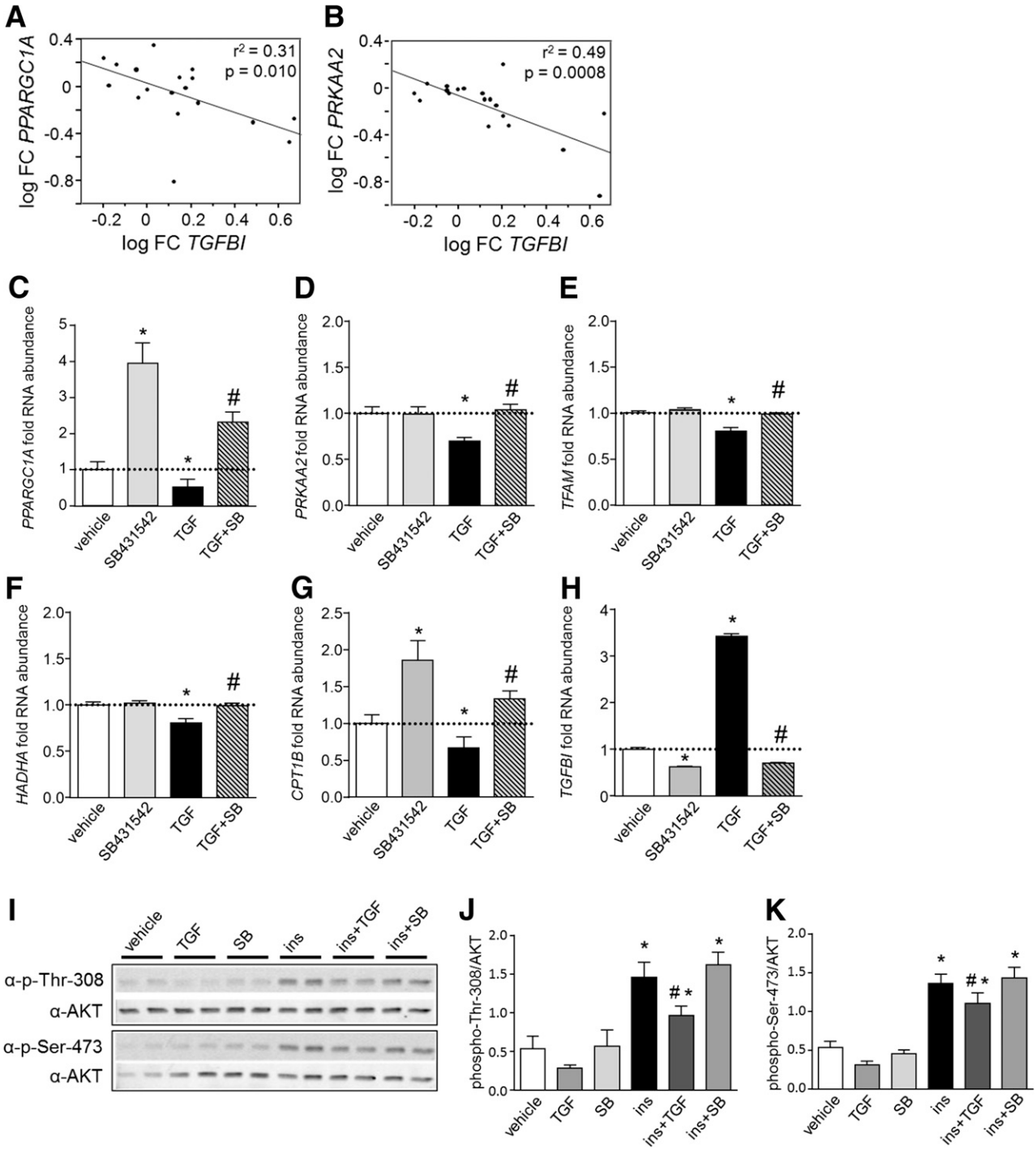

Figure 3—TGF-β1 activity is related to the suppression of mitochondrial regulators in human skeletal muscle. *A* and *B*: Correlation of log-transformed fold changes (FC) (after intervention vs. before intervention) in *PPARGC1A* or *PRKAA2* and *TGFBI* transcripts in muscle biopsies assessed by transcriptome analyses (n = 18). *C–H*: Relative fold change of mRNA abundance of indicated genes related to *TBP* measured by qPCR in fully differentiated human skeletal muscle cells treated with 10 μmol/L SB431542 (SB), 2 ng/mL TGF-β1, or both (TGF+SB) for 24 h. Dotted lines indicate the mean of the vehicle-treated cells set as 1. Shown is the fold change compared with vehicle-treated cells (n = 4, mean ± SD). *P < 0.05 vs. vehicle-treated cells; #P < 0.05 vs. TGF-β1-treated cells. *I–K*: Human skeletal muscle cells were treated with 1 ng/mL TGF-β1 or 10 μmol/L SB431542 for 24 h before stimulation with 10 nmol/L insulin (ins) for 10 min. Representative immunoblots of protein lysates (in duplicate) using the antibodies as indicated and relative band intensity values related to AKT are shown (n = 3–6, mean ± SD). *P < 0.05 vs. vehicle-treated cells; #P < 0.05 vs. insulin-treated cells.

had increased mRNA expression levels of enzymes of mitochondrial oxidation and their upstream regulators (41), while expression levels remained unaltered in individuals who could not improve their glucose control. Although the intervention protocol in that study differs from that of our study in several aspects (a 4-month unsupervised walking

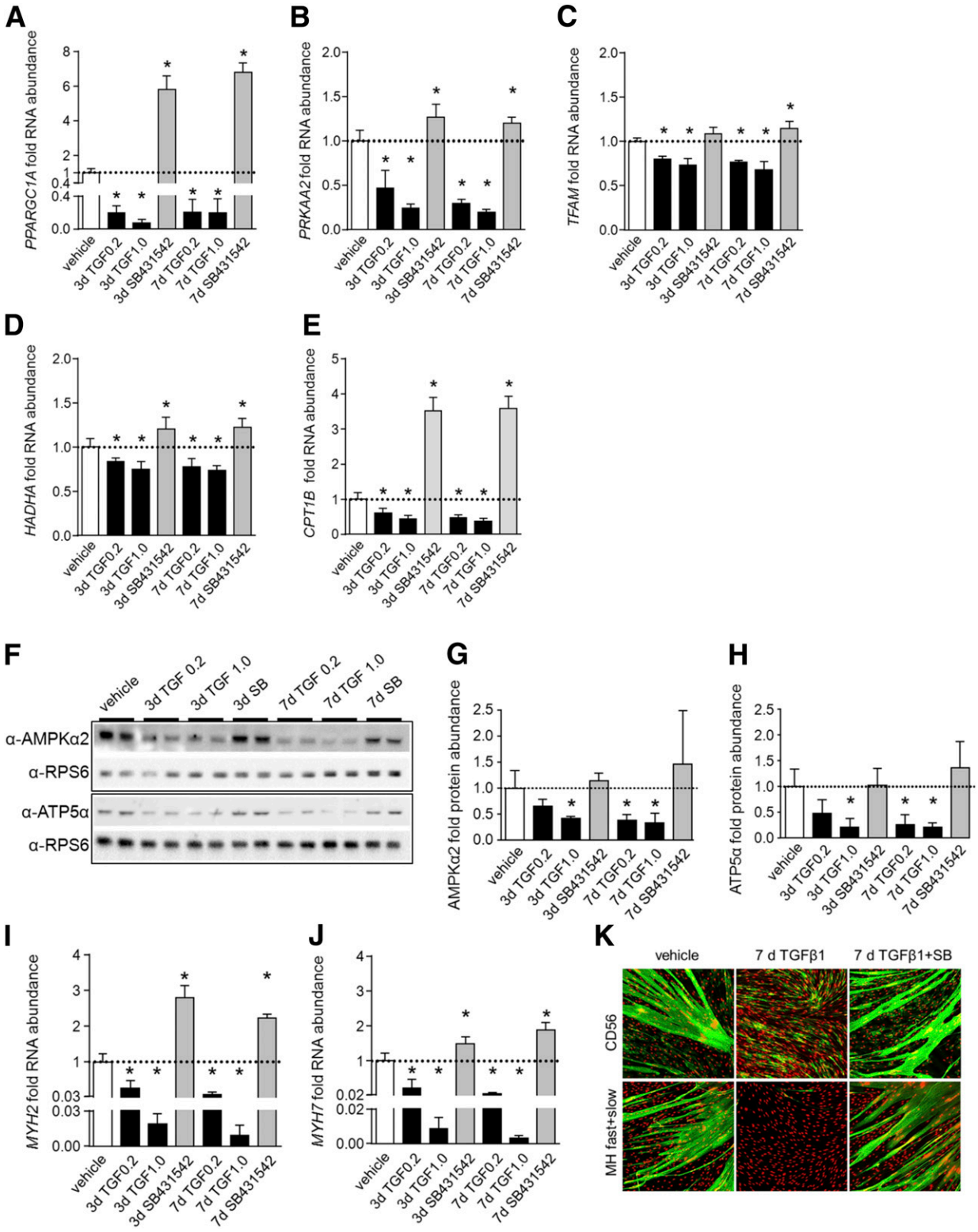

Figure 4—TGF-β1 suppresses mitochondrial regulators and enzymes in human skeletal muscle cells. Human skeletal muscle cells were treated with 0.2 or 1 ng/mL TGF-β1 or 10 μmol/L SB431542 (SB) for 3 or 7 days (d). *A–E*, *I*, and *J*: Relative fold change of mRNA abundance of indicated genes related to *TBP* measured by qPCR. Shown is the fold change compared with vehicle-treated cells (n = 4, mean ± SD). *P < 0.05 vs. vehicle-treated cells. *F–H*: Representative immunoblots of protein lysates (in duplicate) using the indicated antibodies (*F*). Detection of RPS6 served as the loading control of separate blots. Relative band intensity values normalized to RPS6 are shown as fold change compared with vehicle-treated cells (*G* and *H*; n = 4, mean ± SD). *P < 0.05 vs. vehicle-treated cells. *K*: Immunostaining of CD56, MYH2 (fast), and MYH7 (slow) in human skeletal muscle cells treated with 1 ng/mL TGF-β1 or TGF-β1 and 10 μmol/L SB431542 for 7 days. Nuclei are shown in red. Dotted lines indicate the mean of the vehicle-treated cells set as 1.

intervention vs. a 2 months of supervised endurance training), the responders in that study and our HRE group show very similar changes in the expression of metabolic and mitochondrial markers in skeletal muscle.

In conclusion, our data suggest a causal relationship of enhanced TGF-β1 activity in skeletal muscle after training and the suppression of key mitochondrial regulators. The results can contribute to our understanding of the failure of the skeletal muscle to participate in the improvement of insulin sensitivity after exercise intervention. Since skeletal muscle accounts for approximately 30–40% of total body weight in nonobese humans and for more than 85% of insulin-dependent glucose uptake (42), this tissue plays a major role in whole-body metabolic control. Our data underline the importance of personalized training strategies and can, for the first time, open perspectives to target exercise nonresponse by the prevention of dysregulated TGF-β1 signaling in skeletal muscle.

Acknowledgments. The authors thank all study participants. The authors are grateful for the excellent technical support provided by Carina Hermann, Heike Runge, and Lisa Ulmer, as well as the organizational support provided by Louise Fritsche, Jaana Heinze, and Ellen Kollmar, from the University Hospital Tübingen, Tübingen, Germany.

Funding. This study was supported in part by a grant from the German Federal Ministry of Education and Research (Bundesministerium für Bildung und Forschung [BMBF]) (01GI0925) to the German Center for Diabetes Research (DZD e.V.), by grants from the Leibniz Gemeinschaft (SAW-FBN-2013-3) and the Deutsche Forschungsgemeinschaft (DFG) (GRK 1302-2) to C.W., by grants from the Helmholtz-Gemeinschaft Alliance "Imaging and Curing Environmental Metabolic Diseases (ICEMED)" and the Helmholtz Portfolio Theme "Metabolic Dysfunction and Common Disease" to J.B., and by grants from Merck Sharp & Dohme GmbH (Diabetology 2014) and the Deutsche Diabetes Gesellschaft to A.B. The funders had no role in study design, data collection and analysis, decision to publish, or preparation of the manuscript.

Duality of Interest. No potential conflicts of interest relevant to this article were reported.

Author Contributions. A.B., A.F., N.S., A.M.N., H.-U.H., and C.W. conceptualized the study. A.B., C.H., M.I., P.S., G.S., C.S., V.S., J.H., and J.M. performed the investigations. A.B., C.H., M.I., J.M., and C.W. performed the formal analysis. A.B., C.H., M.I., and C.W. wrote the original draft of the article. J.B., A.M.N., H.-U.H., and C.W. reviewed and edited the article. A.B., J.B., M.H.d.A., H.-U.H., and C.W. acquired funding. F.S., J.B., and A.M.N. provided resources. F.S., J.B., M.H.d.A., H.S., A.F., N.S., A.M.N., H.-U.H., and C.W. supervised the study. C.W. is the guarantor of this work and, as such, had full access to all the data in the study and takes responsibility for the integrity of the data and the accuracy of the data analysis.

Prior Presentation. Parts of this study were presented in abstract form at the 76th Scientific Sessions of the American Diabetes Association, New Orleans, LA, 10–14 June 2016.

References

1. Boulé NG, Weisnagel SJ, Lakka TA, et al.; HERITAGE Family Study. Effects of exercise training on glucose homeostasis: the HERITAGE Family Study. Diabetes Care 2005;28:108–114

2. Praet SF, van Loon LJ. Exercise: the brittle cornerstone of type 2 diabetes treatment. Diabetologia 2008;51:398–401

3. Hawley JA. Exercise as a therapeutic intervention for the prevention and treatment of insulin resistance. Diabetes Metab Res Rev 2004;20:383–393

4. Tuomilehto J, Lindström J, Eriksson JG, et al.; Finnish Diabetes Prevention Study Group. Prevention of type 2 diabetes mellitus by changes in lifestyle among subjects with impaired glucose tolerance. N Engl J Med 2001; 344:1343–1350

5. AbouAssi H, Slentz CA, Mikus CR, et al. The effects of aerobic, resistance, and combination training on insulin sensitivity and secretion in overweight adults from STRRIDE AT/RT: a randomized trial. J Appl Physiol (1985) 2015;118:1474–1482

6. Richter EA, Turcotte L, Hespel P, Kiens B. Metabolic responses to exercise. Effects of endurance training and implications for diabetes. Diabetes Care 1992; 15:1767–1776

7. Stephens NA, Sparks LM. Resistance to the beneficial effects of exercise in type 2 diabetes: are some individuals programmed to fail? J Clin Endocrinol Metab 2015;100:43–52

8. Bouchard C, Blair SN, Church TS, et al. Adverse metabolic response to regular exercise: is it a rare or common occurrence? PLoS One 2012;7:e37887

9. Sparks LM, Johannsen NM, Church TS, et al. Nine months of combined training improves ex vivo skeletal muscle metabolism in individuals with type 2 diabetes. J Clin Endocrinol Metab 2013;98:1694–1702

10. Church TS, Blair SN, Cocreham S, et al. Effects of aerobic and resistance training on hemoglobin A1c levels in patients with type 2 diabetes: a randomized controlled trial. JAMA 2010;304:2253–2262

11. Bajpeyi S, Tanner CJ, Slentz CA, et al. Effect of exercise intensity and volume on persistence of insulin sensitivity during training cessation. J Appl Physiol (1985) 2009;106:1079–1085

12. Lakka TA, Rankinen T, Weisnagel SJ, et al. Heritage Family Study. A quantitative trait locus on 7q31 for the changes in plasma insulin in response to exercise training: the HERITAGE Family Study. Diabetes 2003;52:1583–1587

13. Ruchat SM, Rankinen T, Weisnagel SJ, et al. Improvements in glucose homeostasis in response to regular exercise are influenced by the PPARG Pro12Ala variant: results from the HERITAGE Family Study. Diabetologia 2010;53: 679–689

14. Matsuda M, DeFronzo RA. Insulin sensitivity indices obtained from oral glucose tolerance testing: comparison with the euglycemic insulin clamp. Diabetes Care 1999;22:1462–1470

15. Machann J, Thamer C, Schnoedt B, et al. Standardized assessment of whole body adipose tissue topography by MRI. J Magn Reson Imaging 2005;21:455–462

16. Roecker K, Schotte O, Niess AM, Horstmann T, Dickhuth HH. Predicting competition performance in long-distance running by means of a treadmill test. Med Sci Sports Exerc 1998;30:1552–1557

17. Péronnet F, Massicotte D. Table of nonprotein respiratory quotient: an update. Can J Sport Sci 1991;16:23–29

18. Weigert C, Brodbeck K, Staiger H, et al. Palmitate, but not unsaturated fatty acids, induces the expression of interleukin-6 in human myotubes through proteasome-dependent activation of nuclear factor-kappaB. J Biol Chem 2004; 279:23942–23952

19. Wakefield LM, Letterio JJ, Chen T, et al. Transforming growth factor-beta1 circulates in normal human plasma and is unchanged in advanced metastatic breast cancer. Clin Cancer Res 1995;1:129–136

20. Rainer J, Sanchez-Cabo F, Stocker G, Sturn A, Trajanoski Z. CARMAweb: comprehensive R- and bioconductor-based web service for microarray data analysis. Nucleic Acids Res 2006;34:W498–W503

21. Eichner J, Rosenbaum L, Wrzodek C, Häring HU, Zell A, Lehmann R. Integrated enrichment analysis and pathway-centered visualization of metabolomics, proteomics, transcriptomics, and genomics data by using the InCroMAP software. J Chromatogr B Analyt Technol Biomed Life Sci 2014;966: 77–82

22. Wu Z, Puigserver P, Andersson U, et al. Mechanisms controlling mitochondrial biogenesis and respiration through the thermogenic coactivator PGC-1. Cell 1999;98:115–124

23. Egan B, Zierath JR. Exercise metabolism and the molecular regulation of skeletal muscle adaptation. Cell Metab 2013;17:162–184

24. Tiano JP, Springer DA, Rane SG. SMAD3 negatively regulates serum irisin and skeletal muscle FNDC5 and peroxisome proliferator-activated receptor γ coactivator 1-α (PGC-1α) during exercise. J Biol Chem 2015;290:7671–7684

25. Yadav H, Quijano C, Kamaraju AK, et al. Protection from obesity and diabetes by blockade of TGF-β/Smad3 signaling. Cell Metab 2011;14: 67–79
26. Herder C, Zierer A, Koenig W, Roden M, Meisinger C, Thorand B. Transforming growth factor-beta1 and incident type 2 diabetes: results from the MONICA/KORA case-cohort study, 1984–2002. Diabetes Care 2009;32:1921–1923
27. Lessard SJ, Rivas DA, Alves-Wagner AB, et al. Resistance to aerobic exercise training causes metabolic dysfunction and reveals novel exercise-regulated signaling networks. Diabetes 2013;62:2717–2727
28. Massagué J, Cheifetz S, Endo T, Nadal-Ginard B. Type beta transforming growth factor is an inhibitor of myogenic differentiation. Proc Natl Acad Sci U S A 1986;83:8206–8210
29. Kjaer M. Role of extracellular matrix in adaptation of tendon and skeletal muscle to mechanical loading. Physiol Rev 2004;84:649–698
30. Paulsen G, Mikkelsen UR, Raastad T, Peake JM. Leucocytes, cytokines and satellite cells: what role do they play in muscle damage and regeneration following eccentric exercise? Exerc Immunol Rev 2012;18:42–97
31. Neubauer O, Sabapathy S, Ashton KJ, et al. Time course-dependent changes in the transcriptome of human skeletal muscle during recovery from endurance exercise: from inflammation to adaptive remodeling. J Appl Physiol (1985) 2014;116:274–287
32. Mann CJ, Perdiguero E, Kharraz Y, et al. Aberrant repair and fibrosis development in skeletal muscle. Skelet Muscle 2011;1:21
33. Alexakis C, Partridge T, Bou-Gharios G. Implication of the satellite cell in dystrophic muscle fibrosis: a self-perpetuating mechanism of collagen overproduction. Am J Physiol Cell Physiol 2007;293:C661–C669
34. Weigert C, Lehmann R, Hartwig S, Lehr S. The secretome of the working human skeletal muscle–a promising opportunity to combat the metabolic disaster? Proteomics Clin Appl 2014;8:5–18
35. Burks TN, Cohn RD. Role of TGF-β signaling in inherited and acquired myopathies. Skelet Muscle 2011;1:19
36. Danai LV, Flach RJ, Virbasius JV, et al. Inducible deletion of protein kinase Map4k4 in obese mice improves insulin sensitivity in liver and adipose tissues. Mol Cell Biol 2015;35:2356–2365
37. Sartorius T, Staiger H, Ketterer C, et al. Association of common genetic variants in the MAP4K4 locus with prediabetic traits in humans. PLoS One 2012; 7:e47647
38. Handschin C, Chin S, Li P, et al. Skeletal muscle fiber-type switching, exercise intolerance, and myopathy in PGC-1alpha muscle-specific knock-out animals. J Biol Chem 2007;282:30014–30021
39. Pilegaard H, Saltin B, Neufer PD. Exercise induces transient transcriptional activation of the PGC-1alpha gene in human skeletal muscle. J Physiol 2003;546: 851–858
40. Stefan N, Thamer C, Staiger H, et al. Genetic variations in PPARD and PPARGC1A determine mitochondrial function and change in aerobic physical fitness and insulin sensitivity during lifestyle intervention. J Clin Endocrinol Metab 2007;92:1827–1833
41. Osler ME, Fritz T, Caidahl K, Krook A, Zierath JR, Wallberg-Henriksson H. Changes in gene expression in responders and nonresponders to a low-intensity walking intervention. Diabetes Care 2015;38:1154–1160
42. DeFronzo RA, Ferrannini E, Sato Y, Felig P, Wahren J. Synergistic interaction between exercise and insulin on peripheral glucose uptake. J Clin Invest 1981; 68:1468–1474